厚生労働科学研究費補助金
難治性疾患等実用化研究事業（難治性疾患実用化研究事業）

小児重症拡張型心筋症への bridge-to-transplantation/recovery を目指した 骨格筋芽細胞シートの開発と実践

平成 24 年～26 年度　総合研究報告書

研究代表者　澤　芳樹

平成２７（２０１５）年５月

目次

厚生労働科学研究補助金（難治性疾患等実用化研究事業(難治性疾患実用化研究事業)）
総合研究報告書

小児重症拡張型心筋症への bridge-to-transplantation/recovery を目指した骨格筋芽細胞シートの開発と実践

研究代表者
大阪大学大学院医学系研究科　教授　澤　芳樹

研究要旨
既に、成人の心不全患者に対して開発が進められている自己由来骨格筋芽細胞シート移植を、小児重症拡張型心筋症患者へ適応することを目的とする。小児患者に対する本再生細胞治療法の安全性と有効性を検証し、医師主導治験実施と保健医療化を目指し、小児重症心不全患者に対する新たな治療法を確立する。

研究分担者
宮川　繁
大阪大学大学院医学系研究科 特任准教授（常勤）
松山　晃文
大阪大学臨床医工学融合研究教育ｾﾝﾀｰ 招聘教授
早川　堯夫
近畿大学薬学総合研究所　所長

A. 研究目的

小児拡張型心筋症は予後不良な難治性疾患であり、重症例に対しては心臓移植が究極の治療である。2010 年に臓器移植法が改正されたものの、それ以後の小児ドナーからの臓器提供は未だに少なく、心臓移植の実施例は欧米諸国と比べると稀有である。そのため、心臓移植待機期間は長期間におよび、我が国では心臓移植に到達するまでの橋渡しとして、新たな治療法を開発する必要がある。

自己由来骨格筋芽細胞シート移植治療は、当科において既に成人の心不全患者に対する再生治療として開発してきた。本治療法を小児患者に対して応用することにより、小児重症心不全に対する新たな治療戦略を確立することが可能と考えられる。

本研究の目的は、小児重症拡張型心筋症に対する自己由来骨格筋芽細胞シート移植の安全性と有効性を検証し、医師主導治験・保険診療化を目指すことである。

B. 研究方法

1）幼若動物を用いた、骨格筋芽細胞シート移植における安全性と有効性の確認

幼若ミニブタ虚血性心疾患モデルを作成し、骨格筋芽細胞シート移植前後での心機能評価を心臓超音波検査、心臓 MRI 検査を用いて行った。病理組織学的に細胞シート移植前後での検討を行った。それぞれの結果は、成獣動物を用いた同実験結果と比較し、幼若動物での本治療法の効果について検証を行った。

幼若動物から作成した筋芽細胞シートの特性を、免疫染色を用いて成獣動物のものと比較検討した。

本治療法の医師主導治験を実施するため、非臨床安全性試験を実施した。幼若ミニブタ虚血性心疾患モデルに対して、骨格筋芽細胞シート移植前後での心室性不整脈の発生頻度を確認した。心電図解析の方法は、Medtronic 社製植込み型心電計

Reveal®をシート移植前に、モデル動物の前胸部に植込み、プロトコル治療終了後に心電計を取り出し不整脈に発生状況を検証した。

2）骨格筋芽細胞シート移植による小児重症心筋症患者に対する臨床研究

「ヒト幹細胞を用いる臨床研究に関する指針」に沿って、臨床研究計画書作成を行った。

小児重症心筋症患者を対象として、標準的心不全治療を行っても有症状の患者に対して、骨格筋芽細胞シート移植術に基づく再生療法の安全性を評価することを目的とした。選択基準として、1）18歳以下、2）重症心筋症の診断、3）NYHAⅢ度以上の重症心不全、4）左室駆出率 35%以下などの項目を設定した。主要評価項目は、研究期間中の有害事象の発現の有無等の観察で安全性を評価することとした。

3）骨格筋芽細胞シート移植による小児重症拡張型心筋症患者に対する医師主導治験

非臨床試験の終了を見越して、医師主導治験の準備を行った。各種の法令・告示・通知に基づき、実施計画書、治験物概要書の作成を行った。先行する成人患者を対象とした、臨床研究や企業治験で本治療法の安全性と有効性は示されており、保険診療化へ向けた開発が進んでいた。小児患者に対する適応拡大を目指して、再生医療新法に基づき、治験物を GCTP 準拠で作成する準備、実施体制整備を行った。

（倫理面への配慮）

1）動物実験においては、本学動物実験規程に従って行った。

2）臨床研究の実施に際しては、研究計画書、試験薬概要書、手順書など臨床研究に必要な文書は、「ヒト幹細胞を用いる臨床研究に関する指針」を遵守して作成し、院内ヒト幹細胞臨床研究審査委員会での承認を受けた。その後、厚生労働大臣の承認を受け実施を行った。本研究の対象は小児であるために、同意説明には十分に配慮を行い、容易な文章を用いて作成した補助文書（アセント）などを使用し、可能な限り患者本人への説明も十分に行ったうえで、代諾者への informed consent を行い、同意を得て実施した。

3）医師主導治験においては、各種法令・告示・通知に基づき実施し、研究計画書（プロトコール）に関して PMDA での審査、院内治験審査委員会での承認を受け、再生医療新法に基づき実施を予定する。

C. 研究結果

1）幼若動物を用いた、骨格筋芽細胞シート移植における安全性と有効性の確認

幼若動物に対する骨格筋芽細胞シート移植では、治療前後で有意な心機能改善効果を認めた。線維化率の検討等、組織学的検討でも、有意な心機能改善効果を認めた。これらの結果は、成獣動物の結果と比べても、幼若動物での結果の方が有意に心機能改善効果が高い結果が得られた。

幼若動物から作成された骨格筋芽細胞シートからは、成獣動物のものと比べ、HGF、VEGF など、本治療法の中心的役割となるパラクライン効果を示すサイトカイン分泌が有意に多いことが分かった。また、アポトーシス抑制遺伝子の一つである Sirtuin1 蛋白の発現が高率であることが分かった。

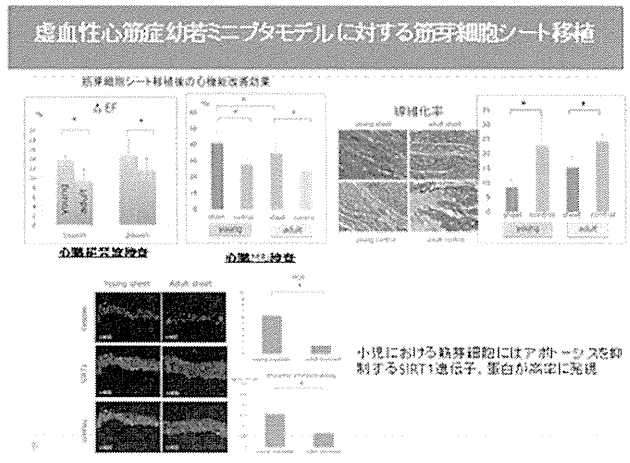

骨格筋芽細胞シート移植に伴う、重篤な有害事象として心室性不整脈の増悪が懸念されているが、幼若ミニブタ虚血性心筋症モデルを用いた筋芽細胞シート移植において、治療前後での心室性不整

脈の発生頻度、重症度に関して、有意な変化は認められなかった。

2）骨格筋芽細胞シート移植による小児重症心筋症患者に対する臨床研究

「ヒト幹細胞を用いる臨床研究に関する指針」を遵守し研究計画書など臨床研究に必要な文書作成を行った。これらは、平成24年11月に実施された大阪大学ヒト幹細胞臨床研究審査委員会において、承認された。その後、厚生労働省へ実施承認申請。平成25年に厚生労働省より実施承認を受けた、小児重症心筋症に対する骨格筋芽細胞シート移植のヒト幹細胞臨床研究（HM1401号）を実施した。プロトコルに沿って、患者選定ならびに1例の被験者登録とシート移植術を施行し、6カ月のフォローアップを終了した。

小児拡張型心筋症患者1例に対して、骨格筋芽細胞シート移植術を行い、プロトコルに沿って6カ月間のフォローアップを完遂した。フォローアップ期間中、シート移植治療が原因となる重篤な有害事象は認めなかった。左室収縮能は、増悪を認めず、拡張能に関しては軽度の改善を認めた。臨床症状の改善（NYHAⅢ度からⅡ度へ）と、6分間歩行において、運動耐容能の改善を認めた。

3）骨格筋芽細胞シート移植による小児重症拡張型心筋症患者に対する医師主導治験

先行する成人を対象とした骨格筋芽細胞シート移植治療は、臨床研究、企業治験、医師主導治験と保険診療化を目指した開発が進行していた。小児患者に対する本治療法の適応拡大をめざし、前述した非臨床試験結果をもとに、医師主導治験実施のための準備を行った。平成26年3月27日に、薬事戦略相談（対面助言）をPMDAと行った。その結果を受け、プロトコルの改正等を行って、平成26年6月16日フォローアップ面談を実施した。非臨床安全性試験を追加する必要がるということで助言を受け、幼若動物を用いた、骨格筋芽細胞シート移植前後での心室性不整脈発生頻度について検証を行った。治験文書の作成、CROとの業務契約締結などを行い、院内IRB申請準備と実施体制の整備を行った。

D.　考察

非臨床安全性試験では、幼若動物において骨格筋芽細胞シート移植治療が、成獣動物のものと比べてより高い心機能改善効果が期待できる可能性が示唆された。組織学的にも結構動態的にも本治療法の有効性を認められた。メカニズムとしては、幼若細胞から作成された筋芽細胞シートから分泌されるサイトカイン量が多いということ、アポトーシスを抑制遺伝子が高率に発現していることが挙げられた。また、骨格筋芽細胞シート移植後に予想される有害事象として、心室性不整脈の増悪があげられるが、細胞シート移植前後で増悪は認められなかった。既に実施されている成人患者に対する本治療法による臨床研究でも、シート移植前後での不整脈の増悪は認められず、その安全性は担保されつつある。小児患者に対する細胞シート移植後も、心室性不整脈が増悪しない可能性が示唆された。

臨床研究では、1例の小児拡張型心筋症患者に対して、本治療法が適応された。細胞シート移植後の6ヵ月フォローアップ期間中、重篤な有害事象は報告されず、安全性を示すことができた。本症例の経時的推移としては、心機能ならびに臨床症状の改善が認められ、有効性も示唆される所見が得られた。安全性及び有効性評価に関しては、さらなる症例数の蓄積が必要であり、今後も被験者選定とリクルートを継続する。

医師主導治験実施を予定しており、実施体制の整備と必要な安全性試験の実施を行うことができた。先行する成人に対する本試験では、テルモ株式会社が企業治験の後に、平成26年11月に薬事承認申請を行っている。これを受け、小児患者に対して本治療法を適応拡大する戦略が現実的となった。平成27年度以降、院内での治験審査委員会での承認、治験届の提出等、治験実施に向けての準備を

継続する予定である。

E. 結論

本研究は、自己骨格筋芽細胞シート治療による新たな小児心不全治療体系の確立を目的として実施された。非臨床試験と臨床研究実施での本治療法の安全性が示唆されたため、今後、医師主導治験へと展開することが可能であり、保険診療化を目指した開発が進むものと思われる。

F. 健康危険情報

該当なし

G.研究発表

1．論文発表

1. Cell-sheet therapy with omentopexy promotes arteriogenesis and improves coronary circulation physiology in failing heart. Kainuma S, Miyagawa S, Fukushima S, Pearson J, Chen YC, Saito A, Harada A, Shiozaki M, Iseoka H, Watabe T, Watabe H, Horitsugi G, Ishibashi M, Ikeda H, Tsuchimochi H, Sonobe T, Fujii Y, Naito H, Umetani K, Shimizu T, Okano T, Kobayashi E, Daimon T, Ueno T, Kuratani T, Toda K, Takakura N, Hatazawa J, Shirai M, Sawa Y. Mol Ther. 2015 Feb;23(2):374-86. doi: 10.1038/mt.2014.225. Epub 2014 Nov 25.

2. Targeted delivery of adipocytokines into the heart by induced adipocyte cell-sheet transplantation yields immune tolerance and functional recovery in autoimmune-associated myocarditis in rats. Kamata S, Miyagawa S, Fukushima S, Imanishi Y, Saito A, Maeda N, Shimomura I, Sawa Y. Circ J. 201;79(1):169-79. doi: 10.1253/circj.CJ-14-0840. Epub 2014 Nov 5.

3. Safety and Efficacy of Autologous Skeletal Myoblast Sheets (TCD-51073) for the Treatment of Severe Chronic Heart Failure due to Ischemic Heart Disease. Sawa Y, Yoshikawa Y, Toda K, Fukushima S, Yamazaki K, Ono M, Sakata Y, Hagiwara N, Kinugawa K, Miyagawa S. Circ J. 2015;79(5):991-9 doi: 10.1253/circj.CJ-15-0243

4. Addition of Mesenchymal Stem Cells Enhances the Therapeutic Effects of Skeletal Myoblast Cell-Sheet Transplantation in a Rat Ischemic Cardiomyopathy Model. Shudo Y, Miyagawa S, Ohkura H, Fukushima S, Saito A, Shiozaki M, Kawaguchi N, Matsuura N, Shimizu T, Okano T, Matsuyama A, Sawa Y. Tissue Eng Part A. 2014;20(3-4):728-39

5. Impact of cardiac stem cell sheet transplantation on myocardial infarction. Alshammary S, Fukushima S, Miyagawa S, Matsuda T, Nishi H, Saito A, Kamata S, Asahara T, Sawa Y. Surg Today. 2013;43(9):970-6

6. Human Cardiac Stem Cells With Reduced Notch Signaling Show Enhanced Therapeutic Potential in a Rat Acute Infarction Model. Matsuda T, Miyagawa S, Fukushima S, Kitagawa-Sakakida S, Akimaru H, Horii-Komatsu M, Kawamoto A, Saito A, Asahara T, Sawa Y. Circ J. 2013;78(1): 222-31

7. Myocardial layer-specific effect of myoblast cell-sheet implantation evaluated by tissue strain imaging. Shudo Y, Miyagawa S, Nakatani S, Fukushima S, Sakaguchi T, Saito A, Asanuma T, Kawaguchi N, Matsuura N, Shimizu T, Okano T, Sawa Y. Circ J. 2013;77(4):1063-72

8. Spatially oriented, temporally sequential smooth muscle cell-endothelial progenitor cell bi-level cell sheet neovascularizes ischemic myocardium.

Shudo Y. Cohen JE, Macarthur JW, Atluri P, Hsiao PF, Yang EC, Fairman AS, Trubelja A, Patel J, Miyagawa S, Sawa Y, Woo YJ. Circulation. 2013;128:S59-68

9. Transplantation of myoblast sheets that secrete the novel peptide SVVYGLR improves cardiac function in failing hearts. Uchinaka A, Kawaguchi N, Hamada Y, Mori S, Miyagawa S, Saito A, Sawa Y, Matsuura N. Cardiovasc Res. 2013;99(1):102-10

10. Tightly regulated and homogeneous transgene expression in human adipose-derived mesenchymal stem cells by lentivirus with tet-off system. Moriyama H, Moriyama M, Sawaragi K, Okura H, Ichinose A, Matsuyama A, Hayakawa T. PLoS ONE. 2013;8(6):e66274

11. Myoblast sheet can prevent the impairment of cardiac diastolic function and late remodeling after left ventricular restoration in ischemic cardiomyopathy. Saito S, Miyagawa S, Sakaguchi T, Imanishi Y, Iseoka H, Nishi H, Yoshikawa Y, Fukushima S, Saito A, Shimizu T, Okano T, Sawa Y. Transplantation. 2012;Jun 15;93(11):1108-15

12. Intracoronary artery transplantation of cardiomyoblast-like cells from human adipose tissue-derived multi-lineage progenitor cells improve left ventricular dysfunction and survival in a swine model of chronic myocardial infarction. Okura H, Saga A, Soeda M, Miyagawa S, Sawa Y, Daimon T, Ichinose A, Matsuyama A. Biochem Biophys Res Commun. 2012;425:859-65

13. Human adipose tissue-derived multilineage progenitor cells exposed to oxidative stress induce neurite outgrowth in PC12 cells through p38 MAPK signaling. Moriyama M, Moriyama H, Ueda A, Nishibata Y, Okura H, Ichinose A, Matsuyama A, Hayakawa T. BMC Cell Biol. 2012;13:21

14. Adipose Tissue-Derived Multi-lineage Progenitor Cells as a Promising Tool for In Situ Stem Cell Therapy. Okura H, Saga A, Soeda M. Ichinose A, Matsuyama A. Current Tissue Engineering. 2012;1:43

15. 再生細胞治療とレギュラトリーサイエンス. 松山晃文. 臨床血液. 2012;53:1801-1807

16. 再生医療とレギュラトリーサイエンス. 大倉華雪, 松山晃文. Medical Science Digest. 2012;39:486-489

17. 再生医療における臨床試験のあり方. 松山晃文. 最新医学. 2012;67:2660-2664

18. 再生医療とレギュラトリーサイエンス. 大倉華雪, 松山晃文. 整形・災害外科. *in press.*

19. Generation of metabolically functioning hepatocytes from human pluripotent stem cells by FOXA2 and HNF1α transduction. Takayama K, Inamura M, Kawabata K, Sugawara M, Kikuchi K, Higuchi M, Nagamoto Y, Watanabe H, Tashiro K, Sakurai F, Hayakawa T, Furue MK, Mizuguchi H. J Hepatol. 2012;Sep;57(3):628-36

20. The promotion of hepatic maturation of human pluripotent stem cells in 3D

co-culture using type I collagen and Swiss 3T3 cell sheets. Nagamoto Y, Tashiro K, Takayama K, Ohashi K, Kawabata K, Sakurai F, Tachibana M, Hayakawa T, Furue MK, Mizuguchi H. Biomaterials. 2012;Jun;33(18):4526-34

21. Promotion of hematopoietic differentiation from mouse induced pluripotent stem cells by transient HoxB4 transduction. Tashiro K, Kawabata K, Omori M, Yamaguchi T, Sakurai F, Katayama K, Hayakawa T, Mizuguchi H. Stem Cell Res. 2012;Mar;8(2): 300-11

22. Efficient Generation of Functional Hepatocytes from Human Embryonic Stem Cells and Induced Pluripotent Stem Cells by HNF4α Transduction. Takayama K, Inamura M, Kawabata K, Katayama K, Higuchi M, Tashiro K, Nonaka A, Sakurai F, Hayakawa T, Furue MK, Mizuguchi H. Mol. Ther. 2012;20(1):127-137

２．学会発表

1. 幼若ブタ虚血性心筋症モデルに対する自己骨格筋芽細胞シート移植の有効性の検討
小澤　秀登、宮川　繁、澤　芳樹、他
第 13 回再生医療学会学術集会 2014. 3. 4 京都

2. Juvenile Skeletal Myoblast Has Greater Therapeutic Potentials Of Regenerative Therapy Than Adult Sheet For Treating Chronic Myocardial Infarction In Infarct Porcine
Ozawa H, Miyagawa S, Sawa Y, et al
American Heart Association Scientific Sessions 2013 11.16-11.20 : Dallas,　USA

H. 知的財産権の出願・登録状況（予定を含む）

１．特許取得　該当なし

２．実用新案登録　該当なし

３．その他　該当なし

別紙４

研究成果の刊行に関する一覧表

雑誌

発表者氏名	論文タイトル名	発表誌名	巻号	ページ	出版年
Kainuma S, Miyagawa S, Fukushima S, Pearson J, Chen YC, Saito A, Harada A, Shiozaki M, Iseoka H, Watabe T, Watabe H, Horitsugi G, Ishibashi M, Ikeda H, Tsuchimochi H, Sonobe T, Fujii Y, Naito H, Umetani K, Shimizu T, Okano T, Kobayashi E, Daimon T, Ueno T, Kuratani T, Toda K, Takakura N, Hatazawa J, Shirai M, Sawa Y.	Cell-sheet therapy with omentopexy promotes arteriogenesis and improves coronary circulation physiology in failing heart.	Mol Ther.	2015Feb;23(2)	374-86	2014Nov 25.
Kamata S, Miyagawa S, Fukushima S, Imanishi Y, Saito A, Maeda N, Shimomura I, Sawa Y.	Targeted delivery of adipocytokines into the heart by induced adipocyte cell-sheet transplantation yields immune tolerance and functional recovery in autoimmune-associated myocarditis in rats.	Circ J.	2015;79(1)	169-79	2015
Yoshiki Sawa, MD, PhD1, Yasushi Yoshikawa, MD, Koichi Toda, MD, PhD1; Satsuki Fukushima MD, PhD1, Kenji Yamazaki, MD, PhD2; Minoru Ono, MD, PhD3; Yasushi Sakata, MD, PhD4; Nobuhisa Hagiwara, MD, PhD5; Koichirou Kinugawa, MD, PhD6; Shigeru Miyagawa, MD, PhD1	Safety and Efficacy of Autologous Skeletal Myoblast Sheets (TCD-51073) for the Treatment of Severe Chronic Heart Failure due to Ischemic Heart Disease.	Circ J.	2015;79(5):	991-9	2015
Shudo Y, Miyagawa S, Ohkura H, Fukushima S, Saito A, Shiozaki M, Kawaguchi N, Matsuura N, Shimizu T, Okano T, Matsuyama A, Sawa Y.	Addition of Mesenchymal Stem Cells Enhances the Therapeutic Effects of Skeletal Myoblast Cell-Sheet Transplantation in a Rat Ischemic Cardiomyopathy Model.	Tissue Eng Part A	20(3-4)	728-39	2014

Alshammary S, Fukushima S, Miyagawa S, Matsuda T, Nishi H, Saito A, Kamata S, Asahara T, Sawa Y.	Impact of cardiac stem cell sheet transplantation on myocardial infarction	Surg Today	43(9)	970-6	2013
Matsuda T, Miyagawa S, Fukushima S, Kitagawa-Sakakida S, Akimaru H, Horii-Komatsu M, Kawamoto A, Saito A, Asahara T, Sawa Y.	Human Cardiac Stem Cells With Reduced Notch Signaling Show Enhanced Therapeutic Potential in a Rat Acute Infarction Model	Circ J	78(1)	222-31	2013
Shudo Y, Miyagawa S, Nakatani S, Fukushima S, Sakaguchi T, Saito A, Asanuma T, Kawaguchi N, Matsuura N, Shimizu T, Okano T, Sawa Y	Myocardial layer-specific effect of myoblast cell-sheet implantation evaluated by tissue strain imaging	Circ J	77(4)	1063-72	2013
Shudo Y. Cohen JE, Macarthur JW, Atluri P, Hsiao PF, Yang EC, Fairman AS, Trubelja A, Patel J, Miyagawa S, Sawa Y, Woo YJ	Spatially oriented, temporally sequential smooth muscle cell-endothelial progenitor cell bi-level cell sheet neovascularizes ischemic myocardium.	Circulation	128	S59-68	2013
Uchinaka A, Kawaguchi N, Hamada Y, Mori S, Miyagawa S, Saito A, Sawa Y, Matsuura N	Transplantation of myoblast sheets that secrete the novel peptide SVVYGLR improves cardiac function in failing hearts	Cardiovasc Res	99(1)	102-10	2013
Moriyama H, Moriyama M, Sawaragi K, Okura H, Ichinose A, Matsuyama A, Hayakawa T	Tightly regulated and homogeneous transgene expression in human adipose-derived mesenchymal stem cells by lentivirus with tet-off system.	PLoS ONE	8(6)	e66274	2013
Saito S, Miyagawa S, Sakaguchi T, Imanishi Y, Iseoka H, Nishi H, Yoshikawa Y, Fukushima S, Saito A, Shimizu T, Okano T, Sawa Y.	Myoblast sheet can prevent the impairment of cardiac diastolic function and late remodeling after left ventricular restoration in ischemic cardiomyopathy.	Transplantation	Jun 15;93(11)	1108-15	2012

Okura H, Saga A, Soeda M, Miyagawa S, Sawa Y, Daimon T, Ichinose A, Matsuyama A.	Intracoronary artery transplantation of cardiomyoblast-like cells from human adipose tissue-derived multi-lineage progenitor cells improve left ventricular dysfunction and survival in a swine model of chronic myocardial infarction.	Biochem Biophys Res Commun	425	859-65.	2012
Moriyama M, Moriyama H, Ueda A, Nishibata Y, Okura H, Ichinose A, Matsuyama A, Hayakawa T.	Human adipose tissue-derived multilineage progenitor cells exposed to oxidative stress induce neurite outgrowth in PC12 cells through p38 MAPK signaling.	BMC Cell Biol.	13	21	2012
Okura H, Saga A, Soeda M. Ichinose A, Matsuyama A.	Adipose Tissue-Derived Multi-lineage Progenitor Cells as a Promising Tool for In Situ Stem Cell Therapy.	Current Tissue Engineering,	1	43	2012
Takayama K, Inamura M, Kawabata K, Sugawara M, Kikuchi K, Higuchi M, Nagamoto Y, Watanabe H, Tashiro K, Sakurai F, Hayakawa T, Furue MK, Mizuguchi H.	Generation of metabolically functioning hepatocytes from human pluripotent stem cells by FOXA2 and HNF1α transduction.	J Hepatol.	Sep;57(3)	628-36	2012
Nagamoto Y, Tashiro K, Takayama K, Ohashi K, Kawabata K, Sakurai F, Tachibana M, Hayakawa T, Furue MK, Mizuguchi H.	The promotion of hepatic maturation of human pluripotent stem cells in 3D co-culture using type I collagen and Swiss 3T3 cell sheets.	Biomaterials.	Jun;33(18)	4526-34	2012
Tashiro K., Kawabata K., Omori M., Yamaguchi T., Sakurai F., Katayama K., Hayakawa T., Mizuguchi H.	Promotion of hematopoietic differentiation from mouse induced pluripotent stem cells by transient HoxB4 transduction.	Stem Cell Res.	Mar;8(2)	300-11	2012

Takayama K, Inamura M., Kawabata K., Katayama K., Higuchi M., Tashiro K., Nonaka A., Sakurai F., Hayakawa T., Furue MK., Mizuguchi H	Efficient Generation of Functional Hepatocytes from Human Embryonic Stem Cells and Induced Pluripotent Stem Cells by HNF4α Transduction.	Mol. Ther.	20(1)	127-137	2012

Cell-sheet Therapy With Omentopexy Promotes Arteriogenesis and Improves Coronary Circulation Physiology in Failing Heart

Satoshi Kainuma[1], Shigeru Miyagawa[1], Satsuki Fukushima[1], James Pearson[2], Yi Ching Chen[2], Atsuhiro Saito[1], Akima Harada[1], Motoko Shiozaki[1], Hiroko Iseoka[1], Tadashi Watabe[3], Hiroshi Watabe[3], Genki Horitsugi[4], Mana Ishibashi[4], Hayato Ikeda[4], Hirotsugu Tsuchimochi[5], Takashi Sonobe[5], Yutaka Fujii[5], Hisamichi Naito[6], Keiji Umetani[7], Tatsuya Shimizu[8], Teruo Okano[8], Eiji Kobayashi[9], Takashi Daimon[10], Takayoshi Ueno[1], Toru Kuratani[1], Koichi Toda[1], Nobuyuki Takakura[6], Jun Hatazawa[4], Mikiyasu Shirai[5] and Yoshiki Sawa[1]

[1]Department of Cardiovascular Surgery, Osaka University Graduate School of Medicine, Osaka, Japan; [2]Monash Biomedical Imaging Facility and Department of Physiology, Monash University, Melbourne, Australia; [3]Department of Molecular Imaging in Medicine, Osaka University Graduate School of Medicine, Osaka, Japan; [4]Department of Nuclear Medicine and Tracer Kinetics, Osaka University Graduate School of Medicine, Osaka, Japan; [5]Department of Cardiac Physiology, National Cerebral and Cardiovascular Center Research Institute, Osaka, Japan; [6]Department of Signal Transduction, Research Institute for Microbial Diseases, Osaka University, Osaka, Japan; [7]Japan Synchrotron Radiation Research Institute, Harima, Japan; [8]Institute of Advanced Biomedical Engineering and Science, Tokyo Women's Medical University, Tokyo, Japan; [9]Division of Organ Replacement Research, Center for Molecular Medicine, Jichi Medical School, Tochigi, Japan; [10]Department of Biostatistics, Hyogo College of Medicine, Hyogo, Japan

Cell-sheet transplantation induces angiogenesis for chronic myocardial infarction (MI), though insufficient capillary maturation and paucity of arteriogenesis may limit its therapeutic effects. Omentum has been used clinically to promote revascularization and healing of ischemic tissues. We hypothesized that cell-sheet transplantation covered with an omentum-flap would effectively establish mature blood vessels and improve coronary microcirculation physiology, enhancing the therapeutic effects of cell-sheet therapy. Rats were divided into four groups after coronary ligation; skeletal myoblast cell-sheet plus omentum-flap (combined), cell-sheet only, omentum-flap only, and sham operation. At 4 weeks after the treatment, the combined group showed attenuated cardiac hypertrophy and fibrosis, and a greater amount of functionally ($CD31^+$/$lectin^+$) and structurally ($CD31^+$/α-SMA^+) mature blood vessels, along with myocardial upregulation of relevant genes. Synchrotron-based microangiography revealed that the combined procedure increased vascularization in resistance arterial vessels with better dilatory responses to endothelium-dependent agents. Serial ^{13}N-ammonia PET showed better global coronary flow reserve in the combined group, mainly attributed to improvement in the basal left ventricle. Consequently, the combined group had sustained improvements in cardiac function parameters and better functional capacity. Cell-sheet transplantation with an omentum-flap better promoted arteriogenesis and improved coronary microcirculation physiology in ischemic myocardium, leading to potent functional recovery in the failing heart.

Received 27 August 2014; accepted 16 November 2014; advance online publication 13 January 2015. doi:10.1038/mt.2014.225

INTRODUCTION

Heart failure following myocardial infarction (MI) is a major cause of death and disability worldwide. Despite advances in drug and device therapy, recovery of cardiac function and prevention of transition to heart failure in MI patients remain unsatisfactory, indicating the need for development of novel therapeutic alternatives.[1] Myocardial regenerative therapy with cell-sheet transplantation has been shown to induce angiogenesis via paracrine effects in a chronic MI model.[2,3] However, the proangiogenic effect of the stand-alone cell-sheet treatment may be insufficient to fully relief ischemia in the chronic MI heart that involves a large territory of the left ventricle (LV), since the coronary inflow of the ischemic/infarct myocardium is dependent upon collateral arteries from other territories.[4,5] In addition, microvascular dysfunction is present in critical chronic MI heart across a wide range of the peripheral coronary tree.[6] This highlights the need for a comprehensive understanding of the mechanism of angiogenesis induced by a cell-sheet therapy in ischemic hearts.

For successful therapeutic neovascularization of ischemic tissues, it is essential to induce robust angiogenic responses (angiogenesis), and establish functionally and structurally mature arterial vascular networks (arteriogenesis) that show long-term stability and control perfusion.[5] Establishment of mature vessels is a complex process that requires several angiogenic factors to stimulate vessel sprouting and remodeling (endothelial tubulogenesis accompanied with a pericyte recruitment) of the primitive vascular network. Endothelial vasodilator function of coronary microvessels (resistance arterial vessels) is also an important determinant of myocardial perfusion in response to increased myocardial oxygen demand, playing a critical role in neovascular therapies.[6–8] The attenuated therapeutic effects observed in the previous clinical trials were caused by multiple factors including

Correspondence: Yoshiki Sawa, Chairman of Department of Cardiovascular Surgery, Osaka University Graduate School of Medicine, 2-2-E1, Yamadaoka, Suita, Osaka 565–0871, Japan. E-mail: sawa-p@surg1.med.osaka-u.ac.jp

generation of unstable blood vessels that regress over time or functionally immature vessels accompanied with endothelial dysfunction in ischemic areas.[5,9]

The omentum (OM), historically used in surgical revascularization for patients with ischemic heart disease, is also known to release a number of angiogenic cytokines and attenuate inflammation.[10–14] In addition, the gastroepiploic artery involved in the OM-flap can play an important role as an extracardiac blood source with high perfusion capacity for developing effective collateral vessels for advanced coronary artery disease. We established a combination strategy of cell-sheet transplantation covered with a pedicle OM-flap in porcine models, allowing us to implant large numbers of cells and improve cell survival.[13,14] However, data are scarce regarding the therapeutic effects of such combined treatment on vessel maturity and coronary microcirculation physiology in ischemic territory. We hypothesized that cell-sheet transplantation with a pedicle OM-flap will better promote arteriogenesis and stabilize blood vessels in ischemic myocardium along with improved coronary microcirculation physiology, consequently enhancing the therapeutic effects of cell-sheet therapy. Herein, we focused on vessel maturation induced by cell-sheet therapy with an OM-flap and evaluated the physiological benefits in coronary microcirculation utilizing modern modalities such as *in vivo* synchrotron-based microangiography and positron emission tomography (PET).

RESULTS

Histological analysis of host myocardium

Four weeks after treatment, myocardial structural components, collagen accumulation and cardiomyocyte hypertrophy, were assessed by hematoxylin-eosin, Masson trichrome, and Periodic acid-Schiff staining ($n = 11$ for each group). LV myocardial structure was better maintained in the combined group as compared with the others (**Figure 1c**). The combined group had a significantly thickened anterior LV wall (anterior wall thickness, control 392 ± 31 versus combined 912 ± 34 versus sheet-only 688 ± 27 versus OM-only 500 ± 28 μm) (**Figure 1d**). That group also had a significantly attenuated collagen accumulation (percent fibrosis, 18 ± 1 versus 8 ± 4 versus 13 ± 6 versus 14 ± 1%, respectively) (**Figure 1e**) and cardiac hypertrophy (myocyte size, 23 ± 1 versus 16 ± 1 versus 20 ± 3 versus 21 ± 2 μm, respectively) (**Figure 1f**) in the peri-infarct regions (ANOVA $P < 0.001$ for all).

Gene expressions in peri-infarct myocardium during acute treatment phase

The myocardial gene expressions related to angiogenesis, vessel maturation, and anti-inflammation were analyzed at 3 days after each treatment using real-time PCR ($n = 6$ for each group). As compared to the others, the combined group showed substantially higher gene expressions of *vascular endothelial growth factor (VEGF)-A*, *VEGF receptor-1*, *VEGF receptor-2*, *Akt-1*, *platelet-derived growth factor (PDGF)-β*, *angiopoietin (Ang)-1*, *Tie-2*, *vascular endothelial (VE)-cadherin*, *platelet endothelial cell adhesion molecule (PECAM)-1*, and *stromal cell-derived factor (SDF)-1* in peri-infarct myocardium at the early stage of transplantation (**Figure 2**).

Vessel recruitment in transplanted cell-sheets and donor cell survial

To evaluate the effect of adding OM-flap to the cell-sheet therapy on the vessel recruitment (angiogenesis) in the transplanted area that should be related to the donor cell survival, we serially assessed the number of functional blood vessels with patent endothelial layers (CD31/lectin double-positive cells) in the transplanted area of the sheet-only and combined groups at 3, 7, and 28 days after each treatment ($n = 6$ for each group and each time point) (**Figure 3a–f**). At 3 days after treatment, in the sheet-only group, several blood vessels were just located at the border between the sheet and infarct area (**Figure 3a**), whereas a large number of functional vessels was detected proximal to the border between the cell-sheet and OM and within the sheet in the combined group (**Figure 3d**), suggesting that the cell-sheet received blood supply directly from the infarct myocardium and OM. Consequently, the combined group had greater numbers of functional blood vessels in the cell-sheet than the sheet-only group at any follow-up point, although both groups showed steady decrease in the number of vessels during the 28 days (**Figure 3g**).

The quantitative assessments of the donor (GFP-positive) cell presence were also serially performed to elucidate the donor cell dynamics in the sheet-only (**Figure 3a–c**) and combined (**Figure 3d–f**) groups. We traced the transplanted donor cells and found that there was no significant difference in the engrafted area at 3 days after transplantation between the groups, while the subsequent changes in each group were apparently distinctive (**Figure 3h**). During the 7days after the treatment, the amount of decrease in the engrafted area was substantially smaller in the combined group than that in the sheet-only group, resulting in 4.3-fold increased retention of donor cells in the former group. This led to the greater donor cell presence in the combined group persistently (at least until day 28), which was consistent with the amount of vessel recruitment in the cell-sheet.

Vessel remodeling and maturation in peri-infarct myocardium

We serially assessed neovascular vessel maturity in peri-infarct areas at 3 ($n = 6$ for each group) and 28 days ($n = 11$ for each group) after treatment (**Figure 4**). Vessel density and structural maturity were quantified as the number of CD31 positive and CD31/α-smooth muscle actin (SMA) double-positive vessels per mm^2, respectively. A maturation index was calculated as the percentage of CD31/α-SMA double-positive vessels to total vessel number. Functionally mature vessels with patent endothelial layers were assessed by lectin injection, which binds uniformly and rapidly to the luminal surface of endothelium, thus labeling patent blood vessels. Vessels positive for CD31 but negative for lectin were regarded as functionally immature and undergoing regression, or that had lost patency.[15,16]

In general, α-SMA signals were located at the outer edges of CD31 staining, indicating pericyte attachment to newly formed endothelium. Three days after treatment, there was no difference in number of CD31-positive cells among the groups, though the combined group showed a trend of greater number of functional blood vessels with patent endothelial layers (CD31/lectin double-positive) and structurally (CD31/α-SMA double-positive) mature vessels, with a higher maturation index (**Figure 4a–g**). Notably, the percentage without lectin staining ($CD31^+$/$lectin^-$) was significantly smaller in the combined group.

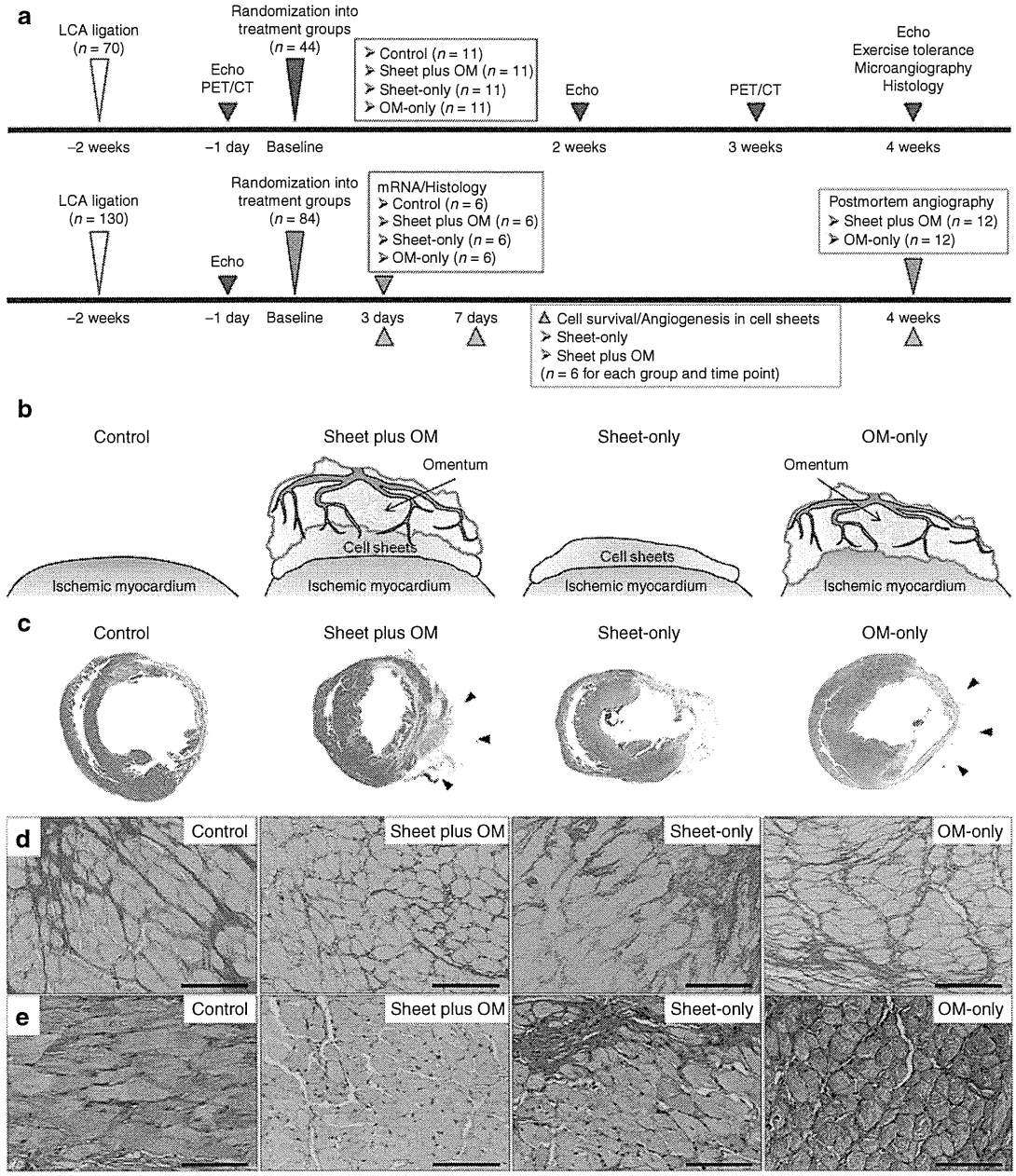

Figure 1 (**a**) Experimental protocols. (**b**) Procedural schemes for treatment groups. (**c**) Macroscopic images of HE-stained whole sections of the left ventricle and (**d**) anterior wall thickness (40×, scale bar = 1,000 μm). Black arrows indicate the omentum tissue. Photomicrographs of Sirius red- (**e**) and periodic acid-Schiff-stained (**f**) sections of peri-infarct myocardium (400×, scale bar = 100 μm) (n = 11 for each group).

The number of endothelial (CD31 positive) cells in the control and single treatment groups decreased with time, while that in the combined remained unchanged. Consequently, the angiogenic effects induced in the latter were more profound at 28 days after treatment, with a significantly greater amount of mature vessels (Figure 4h–n).

Number of resistance vessels and relative dilatory responses to endothelium-dependent stimulation in ischemic myocardium

To evaluate the effects of each treatment on microcirculation physiology in terms of relative dilatory responses to acetylcholine and dobutamine hydrochloride in the resistance vessels, synchrotron radiation microangiography was performed after 3 weeks after the treatment (control: n = 11, combined: n = 11, cell-sheet: n = 5, OM: n = 6). Using iodinated agents, coronary microcirculation in ischemic areas was clearly visualized in anesthetized closed-chest rats (Figure 5a). Vessel internal diameter (ID) at baseline (before agent administration) tended to decrease according to branching order and differed among the groups with larger first branching order arteries observed in the combined group (Figure 5b). Moreover, the combined group had a greater number of third and fourth branching order arterial vessels (resistance arterial vessels) at baseline (Figure 5c).

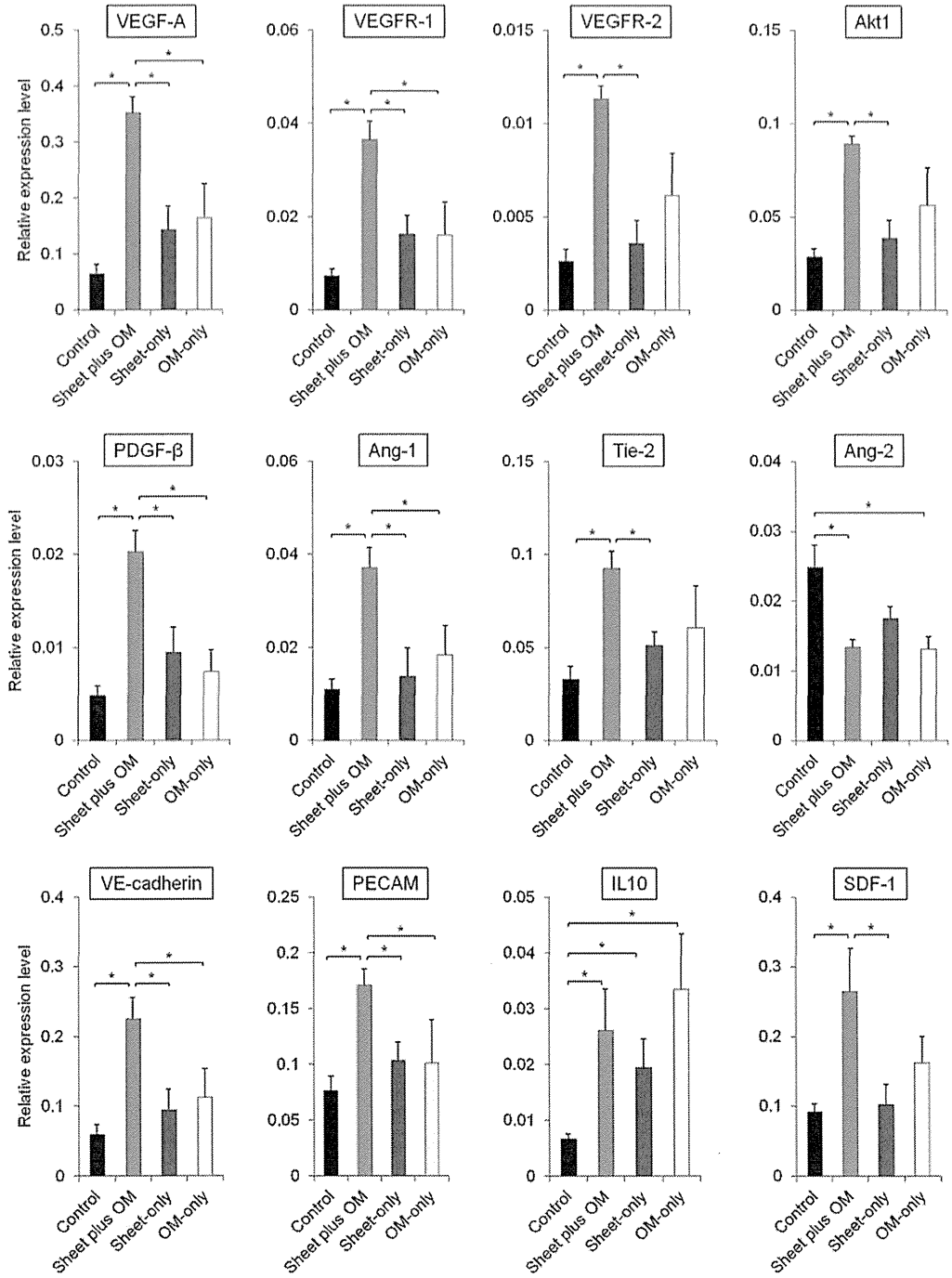

Figure 2 Quantitative reverse transcription PCR showing gene expressions related to angiogenesis, vessel maturation, and anti-inflammation in peri-infarct myocardium 3 days after treatment ($n = 6$ for each group) ($^*P < 0.05$). Data were normalized to β-actin expression level. As compared to the others, the combined group showed substantially higher gene expressions associated with angiogenesis, vessel remodeling and anti-inflammation in peri-infarct myocardium at 3 days after treatment.

Acetylcholine-mediated dilation in the third and fourth branching orders was significantly different among the groups. The mean caliber changes in response to acetylcholine in the combined group were 28±8% and 32±8% for the third and fourth order branches respectively, which were greater than in the others (Figure 5d). Similarly, the mean caliber changes in response to dobutamine hydrochloride in the combined group were 31±7% and 34±7%, respectively, which were greater than in the others (Figure 5e).

The distributions of individual segment caliber changes in response to acetylcholine are described in **Supplementary Figure S1**. The control group had a relatively high frequency of third and fourth branching order arterial vessels showing localized segmental vasoconstriction (ID constriction >5% of baseline). The frequency of abnormal vasoconstriction with acetylcholine in the control group was about eight- and fourfold for the third and fourth branching order, respectively, as compared

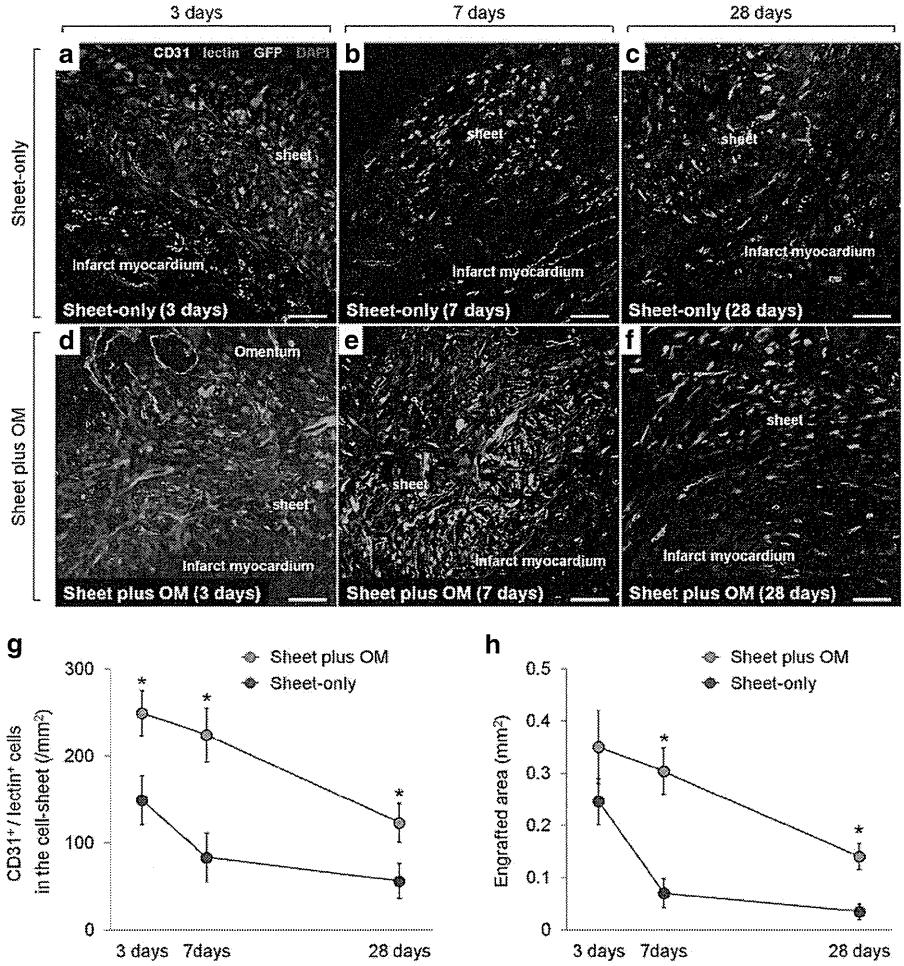

Figure 3 Serial representative images of functional blood vessels with patent endothelial layers (CD31/lectin double-positive) vessels in the transplanted donor (GFP-positive) cells in sheet-only (a–c) and combined groups (d–f) at 3, 7, and 28 days after each treatment (200×, scale bar = 100 μm). Quantitative analyses of functionally mature vessels in the transplanted area (**g**) and the donor (GFP-positive) cell presence (**h**) at 3, 7, and 28 days after each treatment ($n = 6$ for each group and each time point) (* $P < 0.05$ versus sheet-only group). At 3 days after treatment, in the sheet-only group, several blood vessels were just located at the border between the sheet and infarct area (**a**), whereas a large number of functional vessels was detected proximal to the border between the cell-sheet and OM and within the sheet in the combined group (**d**). Consequently, the combined group had greater numbers of functional blood vessels in the cell-sheet than the sheet-only group at any follow-up point (**g**). There was no significant difference in the engrafted area at 3 days after transplantation between the groups, while the subsequent changes in each group were apparently distinctive (**h**). During the 7 days after the treatment, the amount of decrease in the engrafted area was substantially smaller in the combined group than that in the sheet-only group, resulting in 4.3-fold increased retention of donor cells in the former group. This led to the greater donor cell presence in the combined group persistently (at least until day 28), which was consistent with the amount of vessel recruitment in the cell-sheet.

with the combined group (third order: control 49% versus combined 6% versus sheet-only 22% versus OM-only 25%; fourth order: control 18% versus combined 4% versus sheet-only 13% versus OM-only 17%).

Global and regional changes in myocardial blood flow and coronary flow reserve

To evaluate global and regional myocardial blood flow (MBF), and coronary flow reserve (CFR), ^{13}N-ammonia PET measurements were serially performed 1 day before and 3 weeks after the treatments (control: $n = 5$, combined: $n = 8$, cell-sheet: $n = 7$, OM: $n = 7$) (Figure 6a–f). In normal rats used for the validation study, global MBF at rest and during stress was 5.1 ± 0.5 and 7.1 ± 1.3 ml/min/g respectively, while global CFR was 1.4 ± 0.3.

Two weeks after coronary ligation (before treatment), global MBF at rest and during stress were substantially decreased in all groups, with no significant differences. Similarly, global CFR was not different among the groups. Three weeks after treatment, global MBF at rest was not different, while that during stress was significantly greater in the combined and single treatment groups as compared to the control (control 2.5 ± 0.4 versus combined 3.8 ± 0.6 versus sheet-only 3.3 ± 0.5 versus OM-only 3.8 ± 0.3, respectively, ANOVA p=0.0003). Postoperative global CFR was also substantially higher in the treatment groups as compared with the control (control 1.1 ± 0.2 versus combined 1.4 ± 0.2 versus sheet-only 1.4 ± 0.2 versus OM-only 1.4 ± 0.2, respectively, ANOVA p=0.015).

With regard to the magnitude of change in the global CFR (pre- versus post-treatment), the combined group offered the

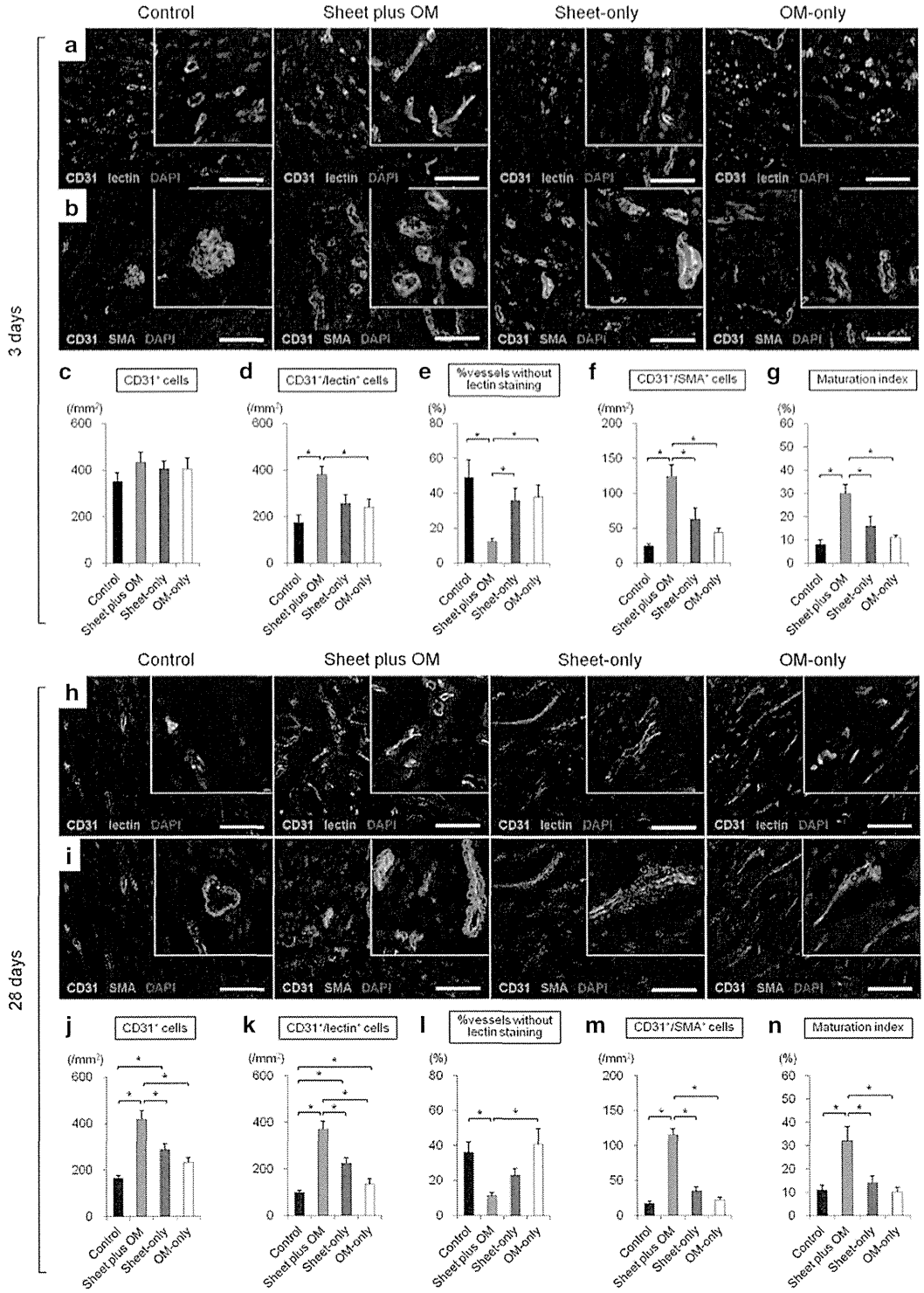

Figure 4 Immunohistochemical analyses of functionality (patency) and vessel maturation observed in peri-infarct myocardium at 3 ($n = 6$ for each group) (**a–g**) and 28 ($n = 11$ for each group) (**h–n**) days after treatments ($^* P < 0.05$). Representative CD31/lectin and CD31/α-SMA staining at 3 (**a,b**) and 28 (**h,i**) days after treatments (400×, scale bar= 100 μm). Three days after treatment, there was no difference in number of CD31-positive cells among the groups, though the combined group showed a trend of greater number of functional blood vessels with patent endothelial layers (CD31/lectin double-positive) and structurally (CD31/α-SMA double-positive) mature vessels, with a higher maturation index (**c–g**). Notably, the percentage without lectin staining ($CD31^+/lectin^-$) was significantly smaller in the combined group. The number of endothelial (CD31 positive) cells in the control and single treatment groups decreased with time, while that in the combined remained unchanged. Consequently, the angiogenic effects induced in the latter were more profound at 28 days after treatment, with a significantly greater amount of mature vessels (**j–n**).

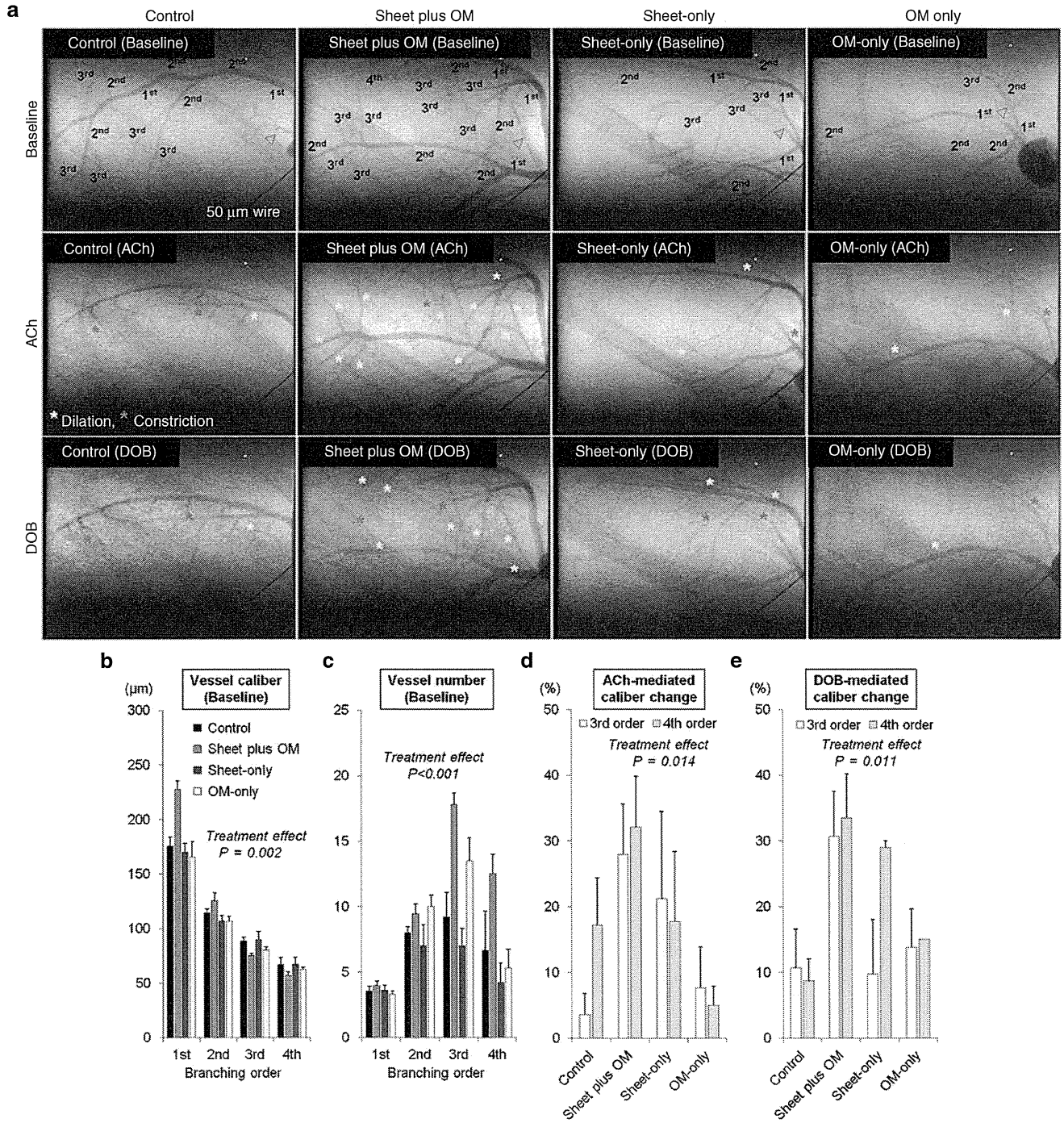

Figure 5 Synchrotron radiation microangiography was performed to evaluate vessel number and caliber and relative dilatory responses to acetylcholine and dobutamine hydrochloride in resistance vessels (control: $n = 11$, combined: $n = 11$, cell-sheet: $n = 5$, OM: $n = 6$). Using iodinated agents, coronary microcirculation in ischemic areas was clearly visualized in anesthetized closed-chest rats. Representative angiogram frames for all treatment groups at baseline, and in response to acetylcholine and dobutamine hydrochloride (**a**). Yellow and red asterisks indicate vessels showing dilation and constriction in response to acetylcholine and dobutamine hydrochloride, respectively. Quantitative analyses of (**b**) vessel internal diameter and (**c**) visible vessel number at baseline according to branching order. Vessel internal diameter at baseline (before agent administration) tended to decrease according to branching order and differed among the groups with larger first branching order arteries observed in the combined group (**b**). Moreover, the combined group had a greater number of third and fourth branching order arterial vessels (resistance arterial vessels) at baseline (**c**). Mean caliber changes in response to (**d**) acetylcholine and (**e**) dobutamine hydrochloride. Acetylcholine-mediated dilation in the third and fourth branching orders was significantly different among the groups. The mean caliber changes in response to acetylcholine in the combined group were 28±8% and 32±8% for the third and fourth order branches respectively, which were greater than in the others (**d**). Similarly, the mean caliber changes in response to dobutamine hydrochloride in the combined group were 31±7% and 34±7%, respectively, which were greater than in the others (**e**).

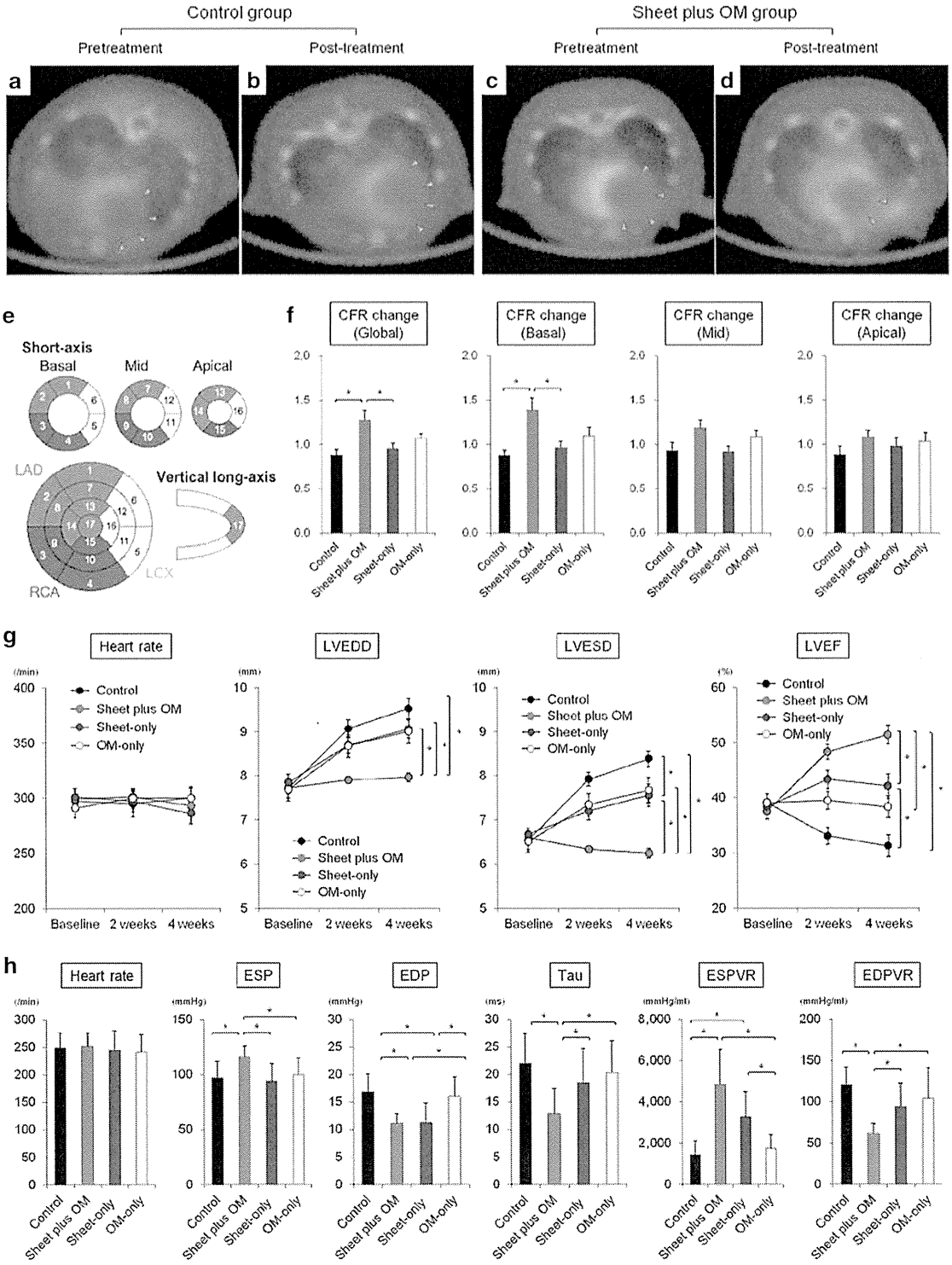

Figure 6 Representative serial PET/CT fusion images of ^{13}N-NH_3 PET during stress in control (a,b) and combined (c,d) groups. Recovery of MBF in large portion of basal left ventricle (anterior and lateral segments) was observed in the combined but not control group (green triangles). Quantitative analyses of changes in CFR calculated as a ratio of post-treatment to pretreatment CFR in global, basal, mid, and apical LV segments (control: $n = 5$, combined: $n = 8$, cell-sheet: $n = 7$, OM: $n = 7$) (*$P < 0.05$) (**e**,**f**). The combined group offered the most remarkable improvement in the global CFR, as evidenced by a higher ratio of post- to pretreatment CFR. Notably, that beneficial change was mainly caused by significant improvement in the basal left ventricle. CFR, coronary flow reserve; MBF, myocardial blood flow. (**g**) Serial assessments of cardiac function parameters at baseline (before treatment), and 2 and 4 weeks after treatments (*$P < 0.05$). In the combined group, remarkable improvements in LV function parameters occurred promptly and were sustained for up to 4 weeks, resulting in significantly smaller LV dimensions and greater LV ejection fraction as compared with other treatment groups. (**h**) Quantitative analyses of hemodynamic function parameters for each treatment (*$P < 0.05$). The basic hemodynamic indices revealed that LV end-systolic pressure was higher, whereas LV end-diastolic pressure and time constant were lower in the combined group as compared to the others. Pressure–volume loop analysis revealed that end-systolic pressure–volume relationship was higher, while end-diastolic pressure–volume relationship was lower in the combined group.